

Journal Pre-proof

Influence of operational modes of the internal heat exchanger in an experimental installation using R-450A and R-513A as replacement alternatives for R-134a

V. Pérez-García, A. Mota-Babiloni, J. Navarro-Esbrí



PII: S0360-5442(19)32043-2

DOI: <https://doi.org/10.1016/j.energy.2019.116348>

Reference: EGY 116348

To appear in: *Energy*

Received Date: 27 June 2019

Revised Date: 2 October 2019

Accepted Date: 12 October 2019

Please cite this article as: Pérez-García V, Mota-Babiloni A, Navarro-Esbrí J, Influence of operational modes of the internal heat exchanger in an experimental installation using R-450A and R-513A as replacement alternatives for R-134a, *Energy* (2019), doi: <https://doi.org/10.1016/j.energy.2019.116348>.

This is a PDF file of an article that has undergone enhancements after acceptance, such as the addition of a cover page and metadata, and formatting for readability, but it is not yet the definitive version of record. This version will undergo additional copyediting, typesetting and review before it is published in its final form, but we are providing this version to give early visibility of the article. Please note that, during the production process, errors may be discovered which could affect the content, and all legal disclaimers that apply to the journal pertain.

© 2019 Published by Elsevier Ltd.

Influence of operational modes of the Internal Heat Exchanger in an experimental installation using R-450A and R-513A as replacement alternatives for R-134a

V. Pérez-García^{*a}, A. Mota-Babiloni^b, J. Navarro-Esbrí^b

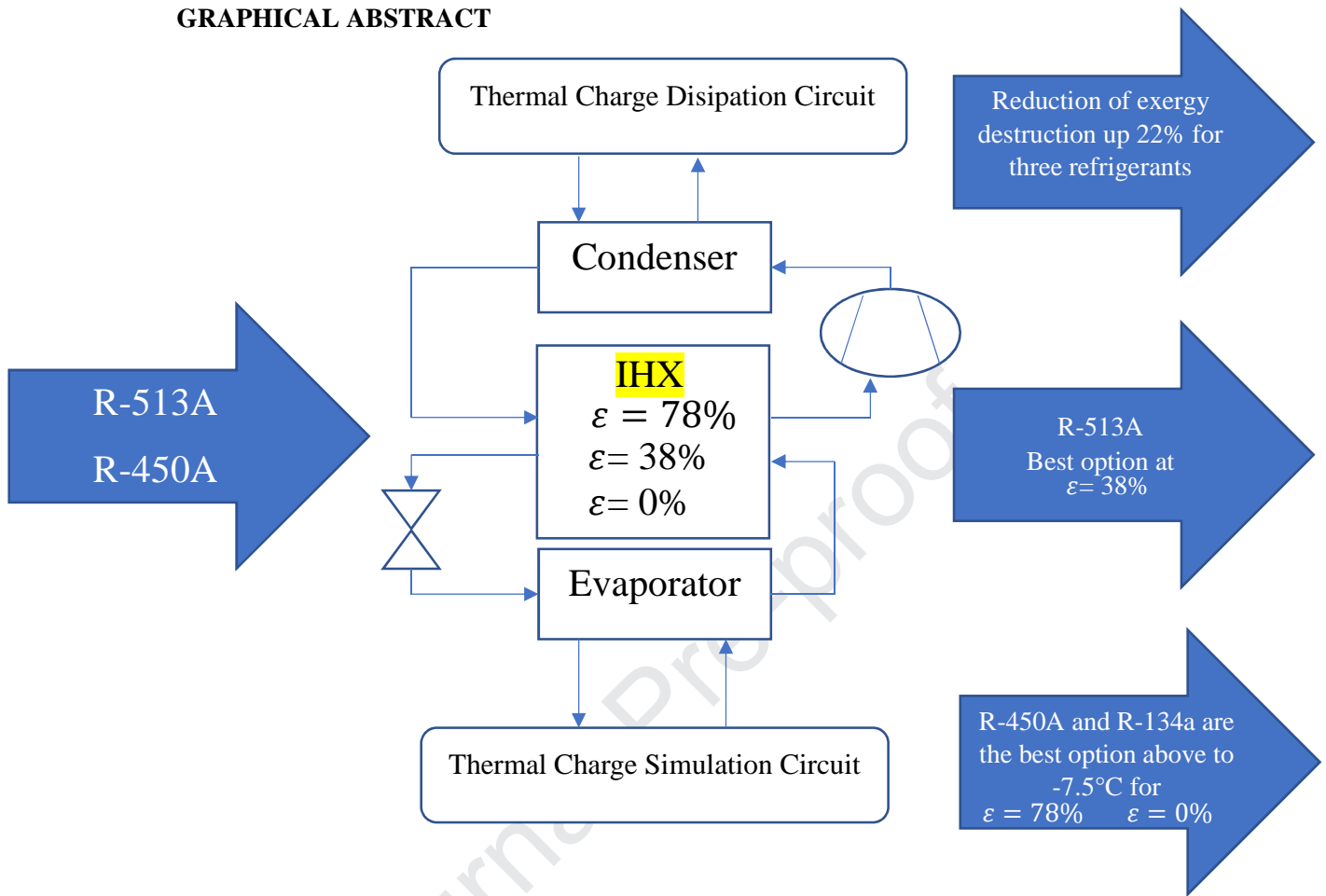
^aUniversity of Guanajuato, Department of Mechanical Engineering, DICIS, Carr. Salamanca-Valle de Santiago, km. 3.5+1.8, Salamanca, Guanajuato, Mexico.

^bISTENER Research Group, Department of Mechanical Engineering and Construction, Universitat Jaume I, Campus de Riu Sec s/n, E12071, Castelló de la Plana, Spain

ABSTRACT

This paper presents a first and second law of Thermodynamic study using experimental data from a medium capacity refrigeration system using R-450A, R-513A and R-134a as working fluids and an internal heat exchanger (IHx) operating in three different modes: disabled (Off), activated at 38% thermal effectiveness (Middle), and activated at 78% thermal effectiveness, which is the maximum value by design (ON). When the IHx is in the Middle mode, R-513A showed to be the best option and its COP overcomes that of R-450A and R-134a. On the other hand, for temperatures above of -7.5°C , both R-450A and R-134a reached the highest COP when the ON and Off modes were set, respectively. Regarding the second law study, for the Off and Middle mode, the largest exergy destruction happens in the compressor for the three refrigerants. The influence of the IHx can be observed directly in the increase of the global exergetic efficiency which passes from being 8.7% in Middle mode to 18.3% for the ON mode. Additionally, a reduction of exergy destruction ratio is seen from the Middle mode, 10.6% to 22.2% in the ON mode.

GRAPHICAL ABSTRACT



Keywords: IHX effectiveness, Exergy destruction, COP, Exergy efficiency

Highlights:

- The use of an IHX in different activation modes produces an increase in the COP
- The activation of an IHX promotes the highest exergy destruction in condenser
- Use of R-513A is suggested only if an IHX is incorporated in a refrigeration cycle
- Use of an IHX can reduce exergy destruction up to 22.2%

Nomenclature

COP	Coefficient of Performance
EDR	Exergy destruction ratio
h	Specific enthalpy (kJ/kg)
I	Irreversibilities (kW)
\dot{m}	Mass flow refrigerant (kg/s)
\dot{Q}	Heat transfer (kW)
s	Specific entropy (kJ/kg K)
T	Temperature (K)
\dot{W}	Power consumption (kW)

Greek symbols

ε	Effectiveness
η	Efficiency

Subscripts

asp	Aspiration
comp	Compressor
cond	Condenser
ev	Expansion valve
evap	Evaporator
g, o	Water/Propylene Glycol outlet
g, i	Water/Propylene Glycol inlet
H	High
i	Inlet
IHX	Internal Heat Exchanger
L	Low
o	Outlet
r	Ideal cycle
ref	Refrigerant
sub	Subcooling
sys	System
w, i	Water inlet
w, o	Water outlet
0	Environmental
II	Second Law

1. INTRODUCTION

Nowadays, the use of hydrofluorocarbons (HFCs) is a common practice for refrigeration and heating, ventilation and air conditioning (HVAC) purposes in most countries of the world. Among them, R-134a is one of the most widely used in domestic refrigeration, supermarkets for food preservation, and chillers [1], despite having a Global Warming Potential (GWP) of 1300 [2]. In this context, the European regulation EU No. 517/2014 [3] has already established a gradual prohibition in the use of refrigerants with high GWP in selected applications. On the other hand, the Kigali agreement [4] also includes a gradual reduction in the use of HFC starting from 2019, which includes developing countries starting between 2024 and 2028.

Under these regulations, low GWP refrigerants must be considered to replace R-134a, without neglecting the importance of keeping energy efficiency high. Among the refrigerants considered as replacement are naturals (CO_2 and hydrocarbons, HCs), hydrofluoroolefins (HFOs) like R-1234yf and R-1234ze(E), and HFC/HFO mixtures like R-450A and R-513A, which presents environmental benefits in comparison with R-134a (see Table 1) . However, except for hydrocarbons, the alternatives above present energy performances (quantified through the coefficient of performance, COP) similar or even under those reached by R-134a. Therefore, to increase the COP in refrigeration systems, different configurations have been implemented, as the basic cycle with an internal heat exchanger (IHx).

Table 1. Environment benefits due to use of R-513A and R-450A versus R-134a [5]

Refrigerant	ODP	GWP	% reduction in GWP
R-134a	0	1300	0
R-450A	0	547	58
R-513A	0	573	56

Currently, different theoretical and experimental works show that the effect of the IHX is positive in terms of the energy performance used in refrigeration systems with both HFCs and HFOs. Pérez-García et al. [6] conducted a study by Second Law on an automotive air conditioning system considering the use of IHX and working with R-1234yf, R-1234ze(E) and R-152a. The results show that R-152a presents a better exergy efficiency when IHX is incorporated into the cycle. Nevertheless, with flammability limits enlisted as 5.1%-17.1% [7], running at high discharge temperatures in the compressor produces high insecurity, according to [8] this refrigerant is not recommended as a direct replacement for R-134a. Mehmet et al. [9] considered the theoretical influence of IHX using R-1234yf and R-134a and demonstrated that this element positively affects the refrigeration capacity because of the subcooling effect. Likewise, their model shows that, under the conditions to which both refrigerants were compared for IHX effectiveness of 50%, the value of the energy performance between both refrigerants is comparable. Navarro-Esbrí et al. [10] experimentally showed that for a vapour compression plant, the replacement of R-134a for R-1234yf reduces the cooling capacity and the COP in 6% and 13%, respectively, but with the inclusion of IHX, these reductions become 2% and 6%, respectively. Mota-Babiloni et al. [11] experimentally concluded that using IHX with effectiveness of 30% produces a positive effect on the refrigerants R-1234yf and R-1234ze(E). Moreover, with IHX, the discharge temperature in these refrigerants keeps a safe range, which is even under the temperature reached by R-134a without IHX. Devecioglu and Oruç [12] compared the energy performance in a refrigeration system using R-1234yf and R-1234ze(E) with the energy performance of R-134a using an IHX. Their results showed that, despite a reduced refrigeration capacity with R-1234ze(E), the energy consumption is also reduced, and comparing it with R-1234yf, the COP of R-1234ze(E) was higher. They also concluded that, with IHX, the COP of the system for R-1234ze(E) was 3% higher than that obtained for R-134a without IHX.

On the other hand, as the R-134a drop-in replacement with pure HFOs cannot be accepted in most cases due to mainly to the COP penalties, HFC/HFO mixtures like R-450A and R-513A have been developed because they show intermediate characteristics between both refrigerant families. Gill et al., [13] conducted an exergy analysis in a refrigeration system without IHX using R-450A as a replacement for R-134a. In comparison with R-134a, the total irreversibility of R-450A was lower, around 15.3% and 27.3%, while the exergy efficiency was higher in 10.1% and 130.1%. Mota-Babiloni et al., [14] performed an exergy study in an experimental installation with R-513A without IHX, demonstrating that the global exergy efficiency of R-513A was slightly higher the one obtained with R-134a under the same operation conditions, though R-513A presented a higher amount of exergy destruction. Yang et al. [15] compared R-513A and R-134a in a domestic refrigerator without IHX and reported that R-513A offers a higher refrigeration capacity in comparison with R-134a. In addition, the discharge temperature in the compressor, as well as the compression ratio, are lower than the ones for R-134a using R-513A. They also evaluated the

energy consumption and found that using R-513A, the energy is reduced by 3.5% in comparison with R-134a. Makhnatch et al. [16] energetically evaluated R-450A and R-513A in comparison with R-134a in an experimental system at higher condensation temperatures. While R-513A surpassed the COP of R-134a in 1.8%, R-450A presented a decrease of 5.3%. Notwithstanding, when the medium condensation temperature is increased from 40°C to 60°C, the COP is significantly reduced, where the refrigerant that shows the highest decrease is R-513A with 36%, while for R-450A, the COP is barely reduced by 35%. López-Belchí [17] numerically and experimentally evaluated a mini-channel condenser with refrigerants R-134a, R-513A and R-1234yf. From a thermal point of view, R-134a reached the best performance in comparison with the other two refrigerants. However, from an environmental point of view, R-134a was the worst option, and therefore R-1234yf was the best option in regions with low CO₂ energy factor and cold climates, and R-513A was the best option only in warm regions with high values of CO₂ energy factors.

Regarding the use of IHX with refrigerants R-450A and R-134a, Mota-Babiloni et al. [18] performed an energy comparison in an experimental installation where they found that the refrigeration capacity is higher for R-134a in comparison with R-450A with and without IHX. Moreover, they reported that the discharge temperature in the compressor is slightly lower for R-450A and the COP varies at a minimum of 0.2% to a maximum of 1.3% for low evaporation temperatures and goes from 0.4% to 2% for high ones, all this considering the installation works with and without IHX. Finally, Mota-Babiloni et al. [19] performed the energy evaluation of R-513A comparing it with R-134a for two operation conditions in the IHX with a 40% effectiveness and another of 80%, where the highest COP is shown when the IHX is activated with an 80% effectiveness. They found that, when the IHX is activated at a 40% effectiveness, the benefits are minimal, but R-513A reaches higher condensation operative conditions with IHX.

There are both theoretical and experimental works focus on determining the exergy in refrigeration systems under different operation conditions for both the evaporator and the condenser using different low GWP refrigerants [8, 20, 21]. Likewise, some researches show the improvement that an IHX produces from the energy and exergy point of view, using alternative refrigerants for R-134a [22-24]. However, works focused in the analysis of the exergy and energy impact on the operation conditions of the IHX based on different effectiveness values with HFC/HFO mixtures as a replacement for R134a have not been found in the literature.

In this work, an energy and exergy analysis is performed for an experimental installation with an IHX that can be activated and deactivated through a set of step valves, depending on what is required. The introduction of this element in the installation influences the exergy destruction in each component. Therefore, the objective of the analysis conducted is to know the impact that the activation of the IHX has for different evaporation temperatures and considering a constant value in the condensation temperature. In addition, this work studies the conditions under the exergy destruction is minimal in the installation, considering 80%, 40% and 0% (when deactivated) effectiveness in the IHX, which are achieved when the valves are completely open, half open, and completely closed, respectively. An energy study is also presented with the aim of showing a complete comparison among the three refrigerants for the mentioned above IHX operation conditions.

2. EXPERIMENTAL PROCEDURE

2.1. Experimental Setup

The experimental tests were conducted in a vapor compression refrigeration installation, which has two secondary circuits to offer the thermal load in the low-pressure stage and the heat dissipation in the high-pressure stage. The installation is completely monitored, and its scheme is shown in Figure 1. Here, the refrigerant enters in the compressor as superheated vapour from internal heat exchanger (1), following, the energy of refrigerant is increasing due to the compression and it exits to high pressure and temperature (2), then enters the condenser to reduce its temperature (3). At the exit of condenser, is placed a coriollis mass flow metter in order to measure the refrigerant mass flow in the installation. Afterwards, when the IHX is used, the refrigerant enters the counter-flow heat exchanger to obtain a sub-cooling effect that will produce an increase in the refrigeration capacity. Subsequently, the refrigerant exits subcooled (4) and enters the expansion valve where it reduces its pressure and goes to the evaporator exit (6). Once the refrigerant leaves the evaporator, IHX enters and additional superheating is produced and sent to the suction compressor (1) where the cycle is repeated. When the IHX is in Off mode, the SV1 and SV3 are closed and SV2 is open and the refrigerant pass directly to the expansion valve (5). Consequently, in this case, SV5 and SV6 are closed too and SV4 is open.

The main components for the installation are the following:

- a) Scroll hermetic compressor with an electric motor of 6.1 kW and a nominal refrigeration capacity of 19.3 kW.
- b) The condenser is a plate heat exchanger with 40 plates and with an exchange area of 2.39 m². In this component, the secondary fluid is water.
- c) The evaporator is a plate heat exchanger with 24 plates and with an exchange area of 1.39 m². This element uses a mixture of water/propylene glycol at 35/65 in percentage volume as secondary fluid.
- d) The IHX is a plate heat exchanger with 30 plates and with an exchange area of 0.336m². The activation of this element is through the opening and closing of passage valves located inside the liquid and aspiration line.
- e) Electronic expansion valve which can be used with R-134a, R-450A and R-513A.

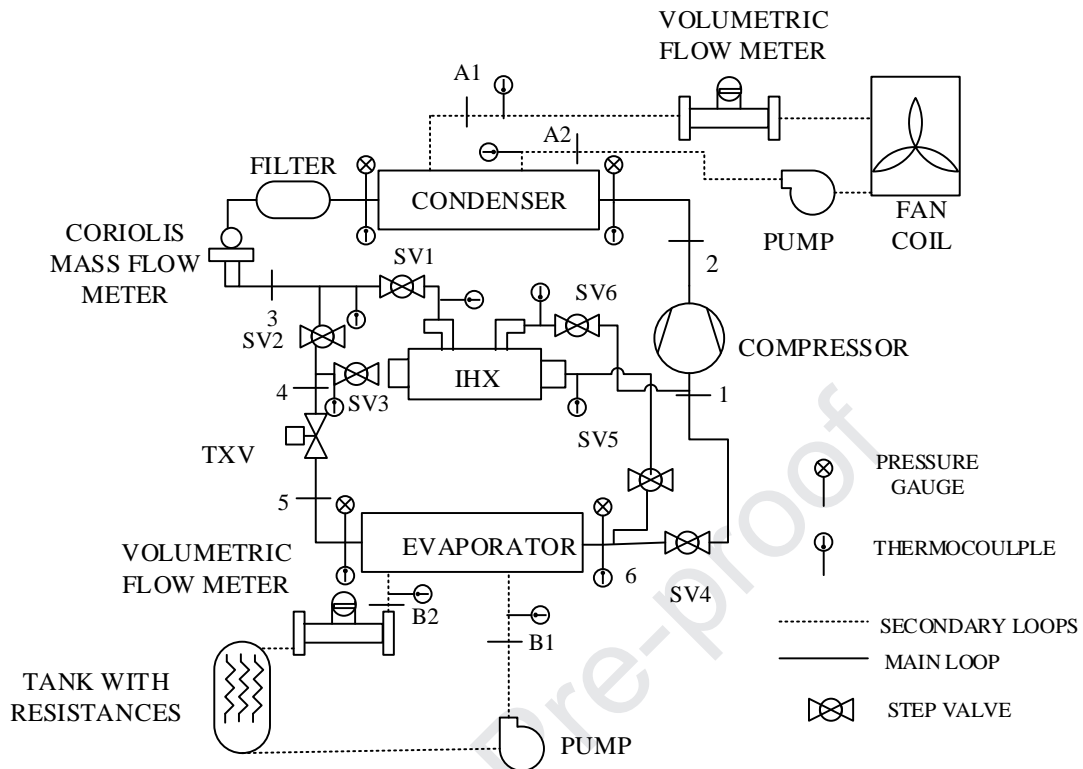


Figure 1. Experimental installation scheme.

The thermal charge dissipation circuit (high-pressure side) uses a water-cooling system through an air heater. Once the water has decreased its temperature (A1), this goes to the secondary side of the installation to produce the refrigerant condensation (A2), while the thermal charge simulation circuit has a tank with resistances which activation is controlled through a PID, here, the glycol mass flow rate flows in direction B2 to B1. In both secondary circuits, the mass flow can be adjusted by using a variable frequency drive for the pumps.

Pressure and temperature sensors are in all the main circuit of the installation, which main characteristics are shown in Table 2. The information obtained with the data acquisition system is processed to determine the thermodynamic state of the refrigerant at the inlet and the outlet from each of the devices, and therefore to calculate its enthalpy and entropy which help to determine the global energy performance and exergy efficiency in the installation. The interface REFPROP v.9.1. [25] was used to determine the thermodynamic properties of the refrigerants. The compressor energy consumption was also measured, as well as the flows in the main and secondary circuits.

Table 2. Uncertainty of sensor in the experimental installation.

Variable	Sensor	Uncertainty
Temperature	Thermocouple	$\pm 0.3\text{K}$
Pressure	Pressure transducer	$\pm 0.15\%$
Refrigerant mass flow rate	Coriolis caudalimeter	$\pm 0.1\%$
Water mass Flow rate	Electromagnetic caudalimeter	$\pm 0.33\%$
Glycol mass Flow rate	Electromagnetic caudalimeter	$\pm 0.114\text{m}^3/\text{hr}$
Compressor Energy consumption	Frequency variator drive	$\pm 1.55\%$

2.2. Test Methodology

The experimental tests were conducted for three levels of operation in the IHX: ON, Middle and OFF. On the ON mode, the refrigerant circulates through the IHX without obstructions, on the Middle mode the step valves are gradually closed until an intermediate effectivity is reached. In the OFF mode, the refrigerant circulates through a bypass, and the valves that provide access to the IHX are close so that this element does not have any influence on the installation. To evaluate the influence of the IHX operation modes on each of the mentioned above operation levels, the tests have been performed on different evaporation temperature values (-15°C, -10°C and -5°C) and a fixed condensation temperature value of 40°C was considered. The superheating was fixed at 10K in the expansion valve, obtaining an average value for this parameter of 10.6K, 11.5K and 12.1K for the refrigerants R-134a, R-450A and R-513A, respectively.

In general, the test performed for each refrigerant lasted for 25 minutes, which is the time in which the thermal stabilization of the installation was achieved. Then, the seven more stable minutes were taken from here to determine the enthalpy and entropy in each of the points where temperature and pressure sensors were located. The data acquisition period was 2 seconds, and therefore, 210 measurements were obtained for each operative point, in which the mentioned above thermodynamic variables were determined.

3. EQUATIONS FOR THE ENERGY AND EXERGY ANALYSIS

The energy and exergy analysis are the tools used to know the energy performance and the irreversibilities presented in a refrigeration system. On the one hand, the energy performance analysis for HFC/HFO mixtures has been studied in a lesser way than it has for pure HFO refrigerants; the works focused on these mixtures are just a few [15,26,27]. On the other hand, the exergy analysis can help to identify the component with higher energy loss, and thus proposing improvements to reduce the existing irreversibilities either in each device or in the system in general. A great variety of theoretical and experimental works use the exergy analysis [13, 28-30]. However, the use of this tool is still limited in the evaluation of HFC/HFO mixtures.

The equations used in the energy as well as the exergy analysis were obtained from energy and exergy balances of each component and are shown in Table 3.

Table 3. Equations for each component in the experimental installation.

Component	Equations for energy performance	Equations for exergy efficiency
Compressor	$\dot{W}_{comp} = \dot{m}_{ref}(h_o - h_i)$	$\dot{I}_{comp} = \dot{m}_{ref}[T_0(s_o - s_i)]$
Condenser	$\dot{Q}_{cond} = \dot{m}_{ref}(h_o - h_i)$	$\dot{I}_{cond} = \dot{m}_{ref}[h_i - T_0s_i - (h_o - T_0s_o)]$
IHX	$\varepsilon = \frac{T_{asp} - T_{evap}}{T_{cond} - T_{evap}}$	$\dot{I}_{IHX} = \dot{m}_{ref}[h_{cond} + h_{evap} - h_{sub} - h_{asp} + T_0(s_{asp} + s_{sub} - s_{cond} - s_{evap})]$
Expansion valve	$h_i = h_o$	$\dot{I}_{ev} = \dot{m}_{ref}T_0(s_o - s_i)$

Evaporator	$\dot{Q}_{evap} = \dot{m}_{ref}(h_o - h_i)$	$i_{evap} = \dot{m}_{ref}T_0 \left[(s_o - s_i) - \left(\frac{h_o - h_i}{T_L} \right) \right]$
------------	---------------------------------------------	-------------------------------------------------------------------------------------------------

Additionally, the COP calculation is performed, as indicated in equation (1).

$$COP = \frac{\dot{Q}_{evap}}{\dot{W}_{comp}} \quad (1)$$

The exergy efficiency in a refrigeration system by vapor compression can be expressed according to equation 2.

$$\eta_{II} = \frac{COP}{COP_r} \quad (2)$$

The COP_r represents the energy performance in the ideal vapor compression cycle in refrigeration mode based on the temperatures of the cold and hot reservoir, equation (3).

$$COP_r = \frac{T_L}{T_H - T_L} \quad (3)$$

Where T_H and T_L can be considered as the average temperature in the heat transfer process, and according to [30], they can be calculated with equations (4) and (5).

$$T_H = \frac{T_{w,o} - T_{w,i}}{\ln\left(\frac{T_{w,o}}{T_{w,i}}\right)} \quad (4)$$

$$T_L = \frac{T_{g,i} - T_{g,o}}{\ln\left(\frac{T_{g,i}}{T_{g,o}}\right)} \quad (5)$$

For the exergy analysis, it is necessary to model the environment in which the system is immersed to obtain a reference state and to determine the exergy losses. The ambient temperature T_0 is a parameter used as a reference for the calculation of the irreversibilities. In this paper, the value of T_0 shows different values, depending on the ambient conditions on the day of the tests. To determine T_0 , the average of the values in this variable was calculated as long as the test lasted, and the results are included in Table 3.

The exergy destruction (irreversibilities) determines the highest energy that can potentially be extracted from the system to produce work. In applications of vapor compression refrigeration, the exergy of product is the exergy of the heat extracted in the evaporator from the space to be cooled, and the exergy of fuel is the actual compressor work input [29]. The energy destruction ratio (EDR) is defined in [29], as equation (6) shows it.

$$EDR = \frac{\text{Total Exergy Destruction}}{\text{Exergy of product}} \quad (6)$$

The total exergy destruction, equation (7), is the addition of the irreversibilities from each component, this is.

$$I_{sys} = I_{comp} + I_{cond} + I_{IHx} + I_{ev} + I_{evap} \quad (7)$$

Additionally, the irreversibilities of each component were calculated according to shown in Table 2.

The EDR can be used as an alternative to evaluating the thermodynamic performance of the system [32], as it is a function of the exergy efficiency, and it is determined through equation (8).

$$EDR = \frac{1}{\eta_{II}} - 1 \quad (8)$$

The equations (1) to (8) and the showed in Table 2, are included in a computational model which is solved through the software, Engineering Equation Solver [33].

4. RESULTS

4.1. T_H , T_L and T_0 temperatures

The experimental results of T_H , T_L y T_0 needed for the calculation of the exergy analysis parameters are shown in Table 4. It shows that the values among the refrigerants studied are close.

Table 4. Experimental values for T_L , T_H and T_0 .

Refrigerant	IHX Operational Mode	Evaporating Temperature (°C)	T_L (K)	T_H (K)	T_0 (K)
R-134a	Off	-5	276.6	310.5	293.9
	Middle		273.2	310.5	294.7
	On		276.8	310.5	294.9
	Off	-10	271.2	311.2	294.4
	Middle		271.4	311.4	296.6
	On		271.2	311.5	296.1
	Off	-15	266.1	311.4	293.8
	Middle		265.7	311.8	294.6
	On		265.4	311.6	294.5
R-450A	Off	-5	276.7	311.1	294.1
	Middle		276.3	311.6	297.6
	On		278.3	312.3	296.1
	Off	-10	272.1	312.1	297.7
	Middle		271.1	312.1	297.3
	On		270.9	311.3	297.7
	Off	-15	267.7	311.3	294.4
	Middle		267.5	312.1	294.3
	On		267.3	312.4	294.6
R-513A	Off	-5	277.4	310.8	291.7

	Middle	-10	276.8	310.9	290.5
	On		277.1	311.2	291.5
	Off		271.8	311.3	292.5
	Middle	-15	271.9	311.5	291.7
	On		272.1	311.8	293.5
	Off		266.7	311.8	293.9
	Middle		267.1	312.1	293.3
	On		267.4	312.3	293.6

4.2. IHX effectiveness

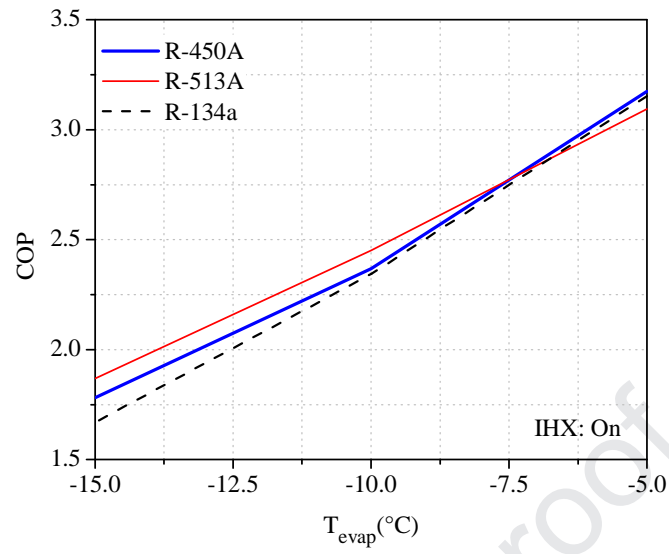
Based on the IHX operation levels, the first parameter evaluated is the effectiveness of this component. In this regard, Table 5 shows the effectiveness values obtained experimentally for each refrigerant. The effectiveness in the On mode varies between 76.1% and 81.2%, obtaining lower variations among refrigerants. The effectiveness in the Middle mode also varies slightly and it can be concluded that the control at the valves has been appropriated.

Table 5. Experimental values of IHX effectiveness to different operational modes.

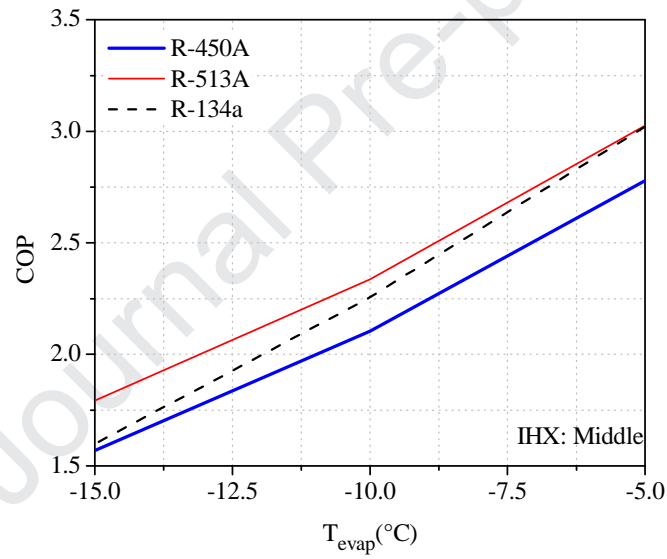
IHX operational mode	Condition	Parameter	R-134a	R-450A	R-513A	Average
Middle	$T_{eva}=-10^{\circ}\text{C}$, $T_{con}=40^{\circ}\text{C}$	ϵ	38.7%	40.4%	39.5%	39.5%
	$T_{eva}=-5^{\circ}\text{C}$, $T_{con}=40^{\circ}\text{C}$		39.3%	39.8%	40.4%	39.8%
	$T_{eva}=-15^{\circ}\text{C}$, $T_{con}=40^{\circ}\text{C}$		42.6%	40.2%	39.9%	40.9%
On	$T_{eva}=-10^{\circ}\text{C}$, $T_{con}=40^{\circ}\text{C}$		81.2%	81.2%	78.2%	80.2%
	$T_{eva}=-5^{\circ}\text{C}$, $T_{con}=40^{\circ}\text{C}$		78.7%	78.5%	76.1%	77.8%
	$T_{eva}=-15^{\circ}\text{C}$, $T_{con}=40^{\circ}\text{C}$		79.5%	79.7%	80.4%	79.3%

4.3. Influence of the IHX operational modes in the COP

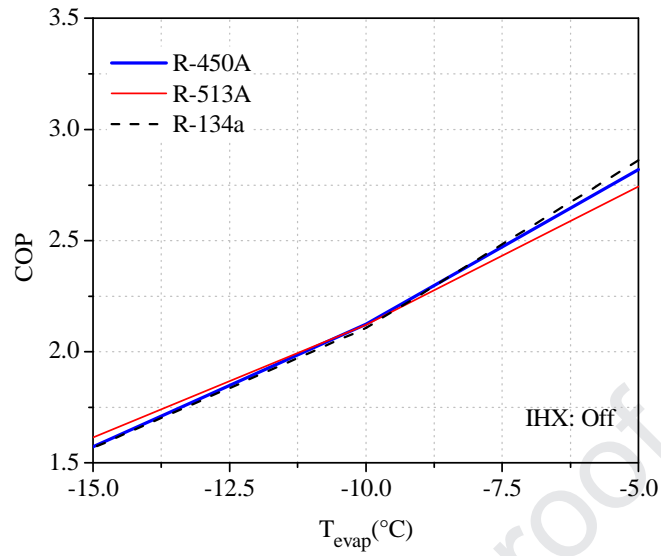
Based on each IHX operation mode, Figure 2 shows the COP variation versus the evaporation temperature for each refrigerant. As the evaporation temperature is increased, the work in the compressor is reduced, and the COP increases (Figure 2c)). On the other hand, if an IHX is introduced, it produces an additional subcooling at the outlet of the condenser, which equally increases the refrigeration capacity. The increase in the evaporation temperature produces a higher heat exchange in the IHX, and the COP tends to increase in any of the operation modes, Middle and ON, as it is showed in Figures 2a) and 2b).



a)



b)

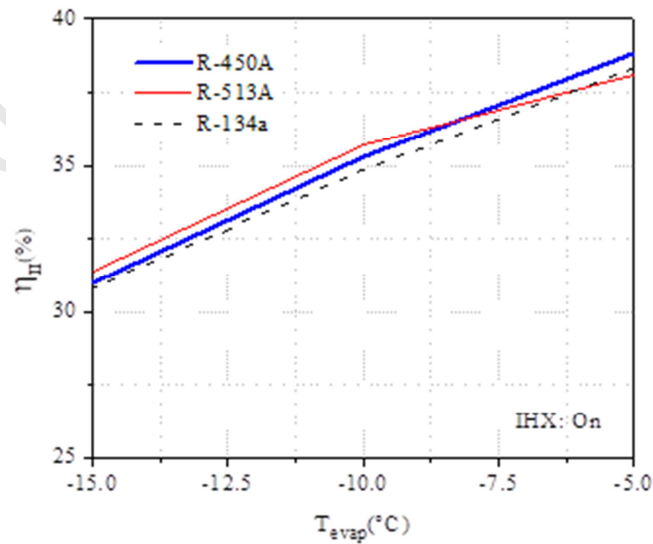


c)

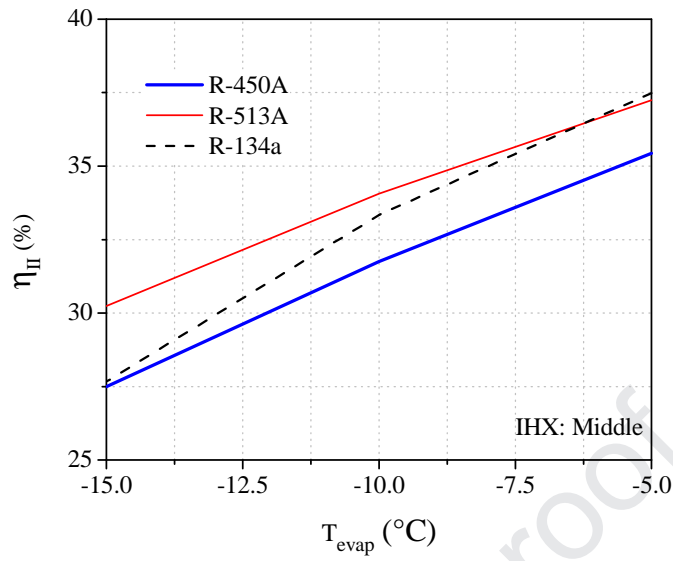
Figure 2. Behavior of COP vs evaporation temperature for the three operational modes in IHX

4.4. Exergy efficiency

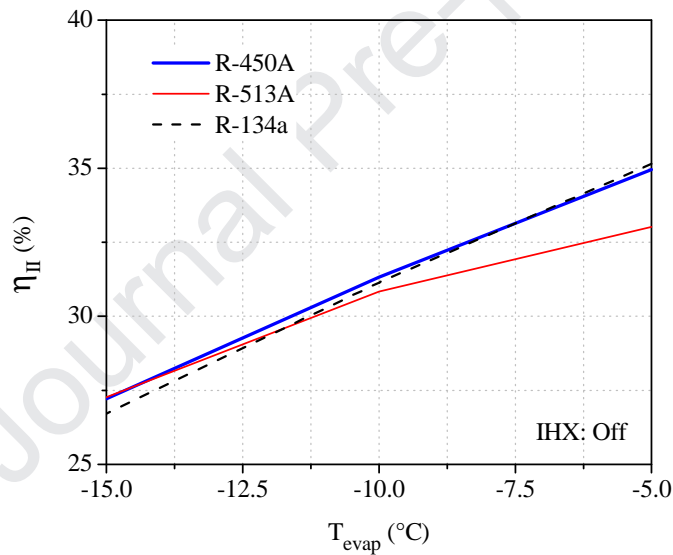
Figure 3 shows the exergy efficiency from the system for each operation mode in the IHX. As the evaporation temperature is increased from -15°C to -5°C , the temperature in the water/ propylene glycol is increased, while the temperature in the water is decreased. This variation causes the temperature gradient $T_H - T_L$ to reduce, and therefore, the exergy efficiency tends to increase. The mentioned above behavior is observed on all the other cases shown.



a)



b)

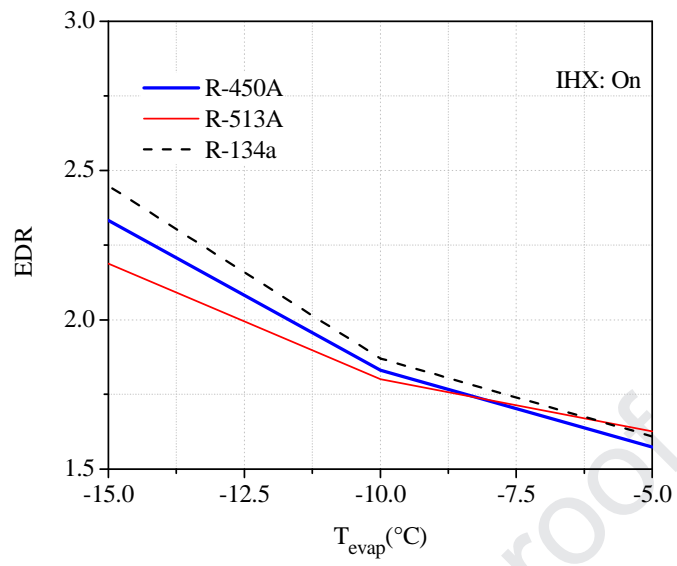


c)

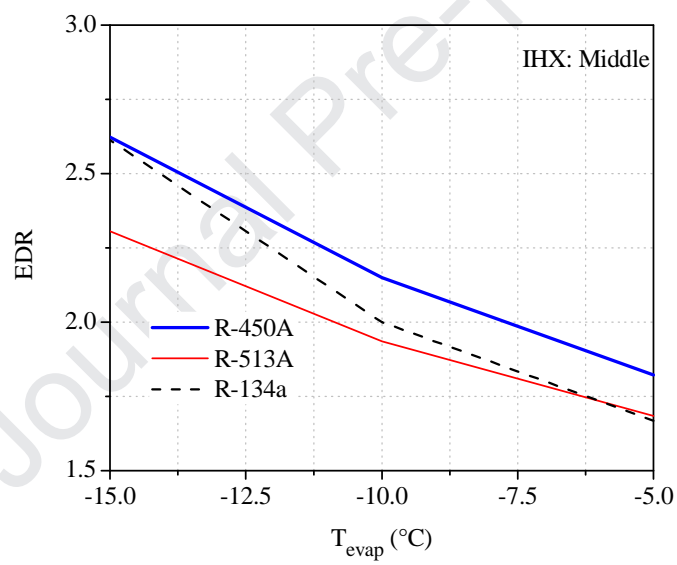
Figure 3. Evolution of exergy efficiency for the three operational modes in the installation.

4.5. Exergy destruction

Figure 4 shows the EDR for all the different operation levels in the IHX. A general reduction of the EDR is observed in the three IHX operation levels as the evaporation temperature is increased. The increase in the evaporation temperature produces not only an increase in the entropy change in the evaporator, but also the temperature in the cold reservoir T_L is increased, which directly affects the irreversibility in the evaporator.



a)



b)

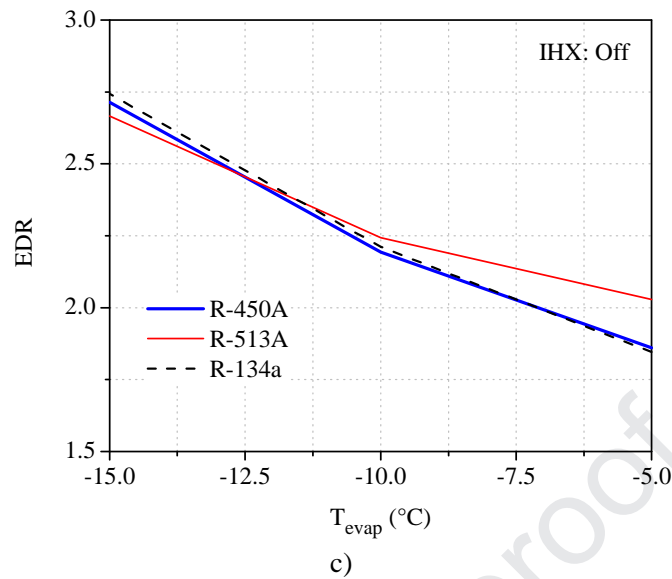


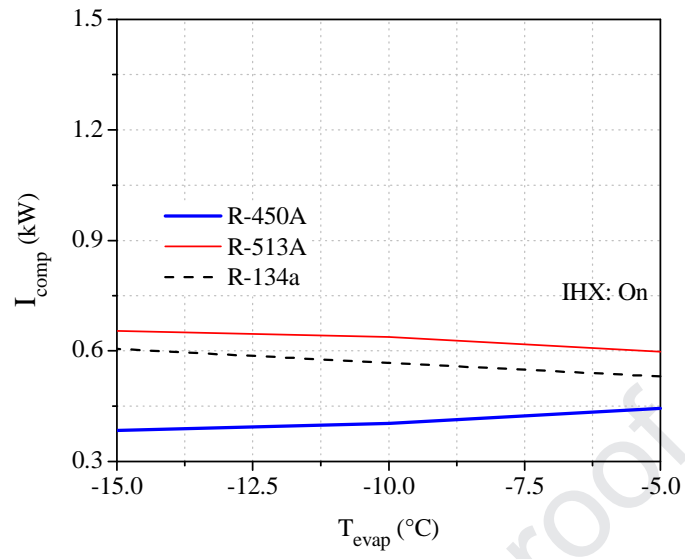
Figure 4. Behavior of exergy destruction ratio in the installation.

4.6. Irreversibilities by component

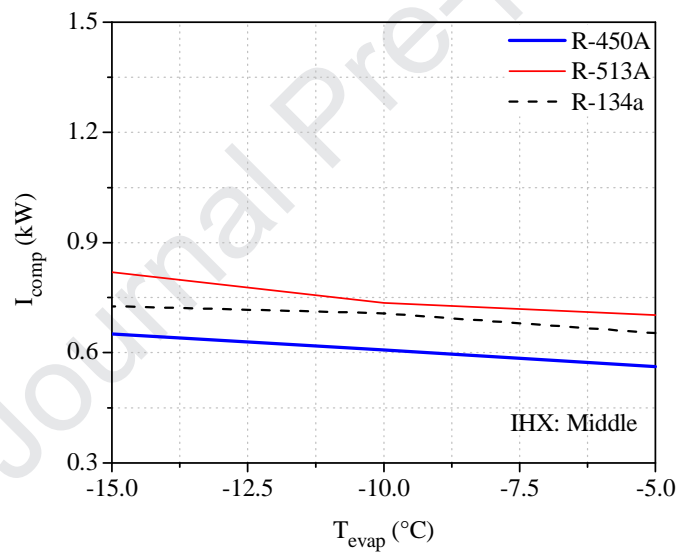
Figures 5 to 9 show the evolution of the irreversibilities in each component and for each IHX operation level.

Figure 5a) shows the influence that the operation mode has on the compressor concerning the evaporation temperature. The irreversibility is increased for this component in 13.4% for the refrigerant R-450A, while for R-134a and R-513A it is reduced by 12.4% and 8.5%, respectively. These behaviors occur because the superheating caused by the IHX in ON mode for R-450A is lower than it is for R-134a and R-513A. Moreover, the discharge temperature for R-450A is higher than those obtained by the other two refrigerants at the same IHX operation mode. Figure 5b) shows that in the Middle mode, the irreversibilities in the compressor are reduced for the three refrigerants. R-513A shows the highest reduction in this parameter with 14.2%, followed by R-450A with 13.6% and finally R-134a with 10%. The irreversibilities reduction for this IHX operation mode occurs because, as the evaporation temperature increases, the overheating degree, as well as the discharge temperature in the compressor, are reduced which causes the entropy increase to diminish, and thus the irreversibility.

Figure 5c) shows that, in OFF mode, the compressor irreversibilities using R-450A are barely reduced 1%, while for refrigerants R-134a and R-513A the increase of this parameter is 7.7% and 8.2%, respectively. The reduction in the irreversibility for R-450A occurs because, as the evaporation temperature increases, a minimal decrease of the entropy in the suction is observed, while the discharge temperature is reduced in magnitude. The increase for R-134a and R-513A occurs because the refrigerants experience a reduction higher in magnitude in the discharge temperature in comparison with R-450A. Furthermore, superheating is minimal in the suction, and this produces a variation in the entropy, which is negligible.



a)



b)

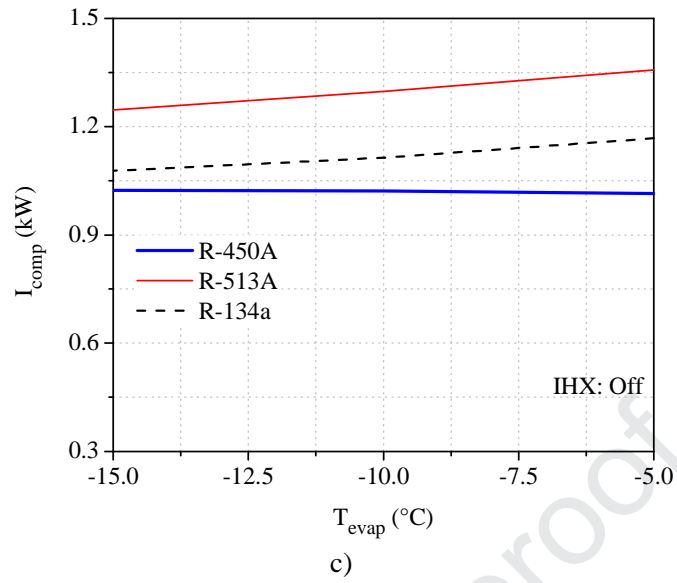
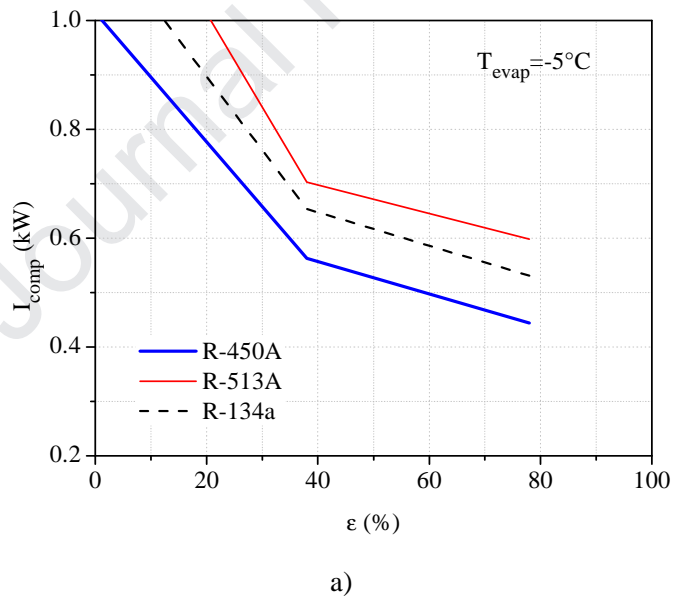
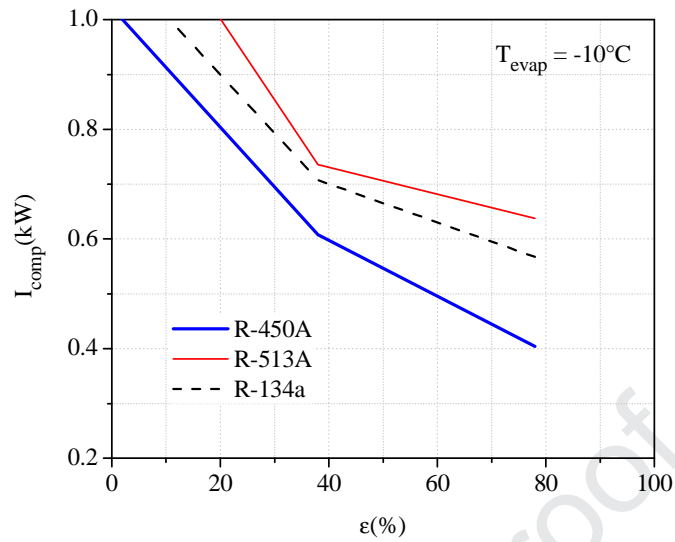


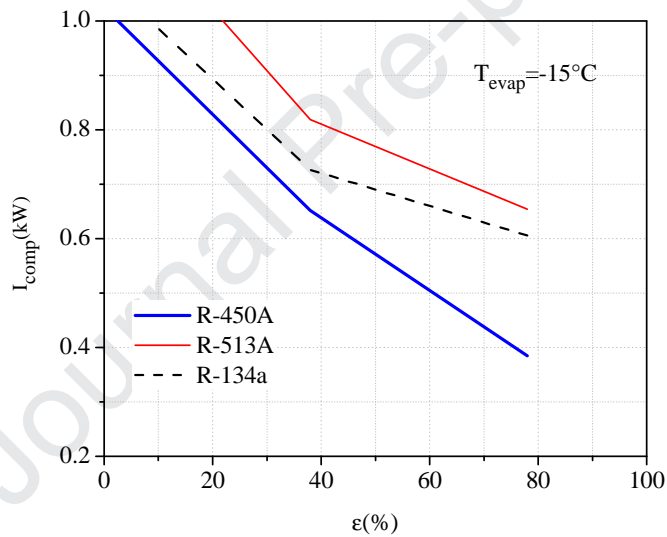
Figure 5. Irreversibilities in the compressor for the three operational modes of IHX.

On the other hand, in Figure 5 it can be appreciate that the increase of the IHX effectiveness produce the reduction of irreversibilities. The above is shown in the Figure 6 and occurs independently of the evaporating temperature.





b)



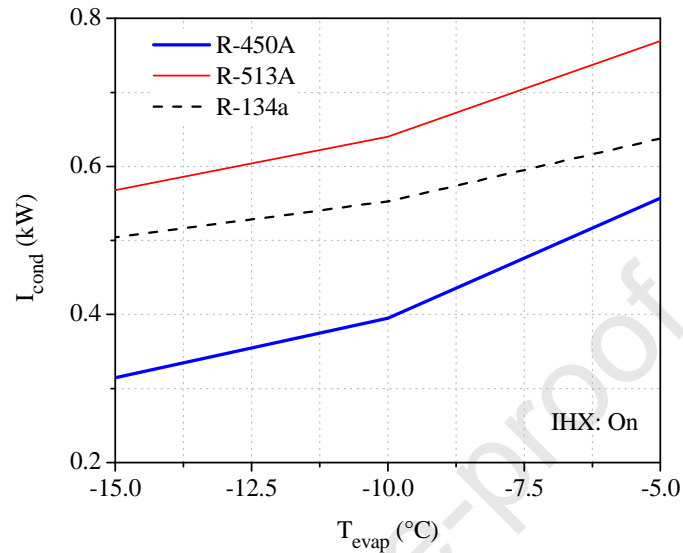
c)

Figure 6. Variation of Irreversibilities vs IHX effectiveness.

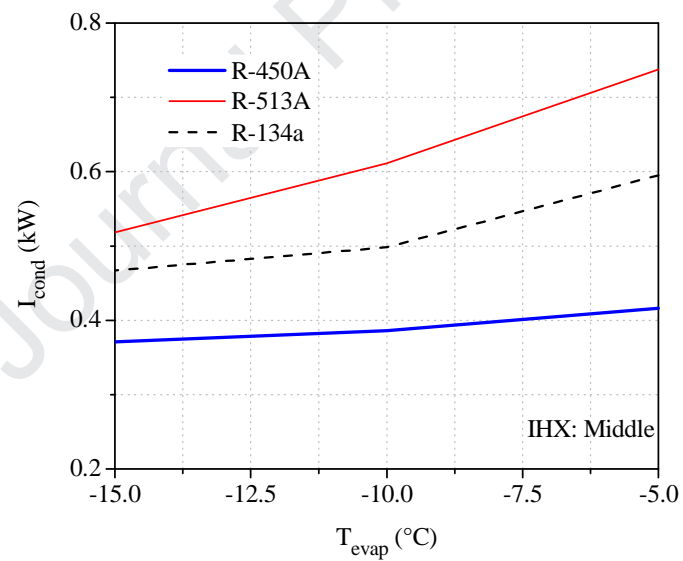
Figure 7 shows the behavior of the irreversibilities in the condenser. In all cases, the irreversibilities increase independently from the IHX operation mode. As the evaporation temperature increases, the exergy at the inlet of the condenser is reduced and considering that the target temperature in this component is the same (40°C), the exergy at the outlet is practically constant. Figure 7a) shows that the highest increase in the irreversibility is for R-450A with 43.5% while for R-134a and R-513A, it increases 20.9% and 26.2%, respectively. When the IHX works in Middle mode (Figure 7b), the irreversibilities equally increase in the condenser for the three refrigerants, however, in this operation mode R-450A is the one which shows the lowest increase in the irreversibility with barely 14.8% in comparison with 21.5% and 29.7% in R-134a and R-513A, respectively.

Figure 7c) shows that the irreversibility in both R-134a and R-513A is very similar at a temperature of -15°C, while the value for this same parameter in R-450A is 32.2% lower at the same

evaporation temperature. In addition, when the IHX is not working in the cycle, R-134a shows the lowest reduction in the irreversibilities for the condenser, while R-450A reaches the highest reduction in this parameter with 37.8% in comparison with 31.6% for R-513A.



a)



b)

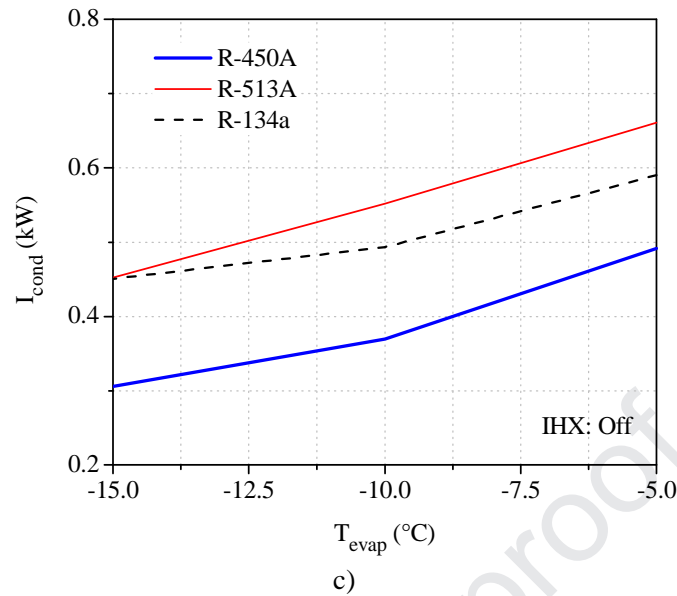


Figure 7. Irreversibilities in the condenser for the three operational modes of IHX.

Figure 8 shows the irreversibilities in the IHX; the ON and Middle modes are the only ones considered for each refrigerant. Figure 8a) presents the evolution of the irreversibilities when the IHX is completely activated. It shows that the refrigerant which produces the highest irreversibility in the IHX is R-513A, where R-450A is the one that presents a lower value in magnitude. The increases in the irreversibility for each refrigerant are 16.1%, 26.7% and 24.2% for R-134a, R-450A and R-513A, respectively.

Figure 8b) shows the behavior of the irreversibility in the IHX when it is working in Middle mode. The refrigerant R-450A presents a considerable increase in the irreversibility concerning R-134a and R-513A. It is showed how at temperatures lower than -10°C , R-450A produces lower irreversibilities in the IHX than those produced by R-513A. The global increase in the irreversibilities is 29.6%, 64.9% and 23.4% for R-134a, R-450A, R-513A, respectively. Particullary, for R-450A from -10°C to -5°C the entropy change increases at double in comparison with the other refrigerants, being this the main reason which the R-450A presents the larger irreversibility. The increase of irreversibilities in the IHX occurs because, as the evaporation temperature increases, the subcooling produced by the IHX in the high-pressure stage is reduced for the three refrigerants. At the same time, the superheating in the low-pressure stage is reduced in the refrigerants R-134a and R-513A, while for R-450A this parameter is increased. Both the subcooling effect and the superheating effect cause the irreversibilities to increase, and for R-450A, the increase is particularly higher.

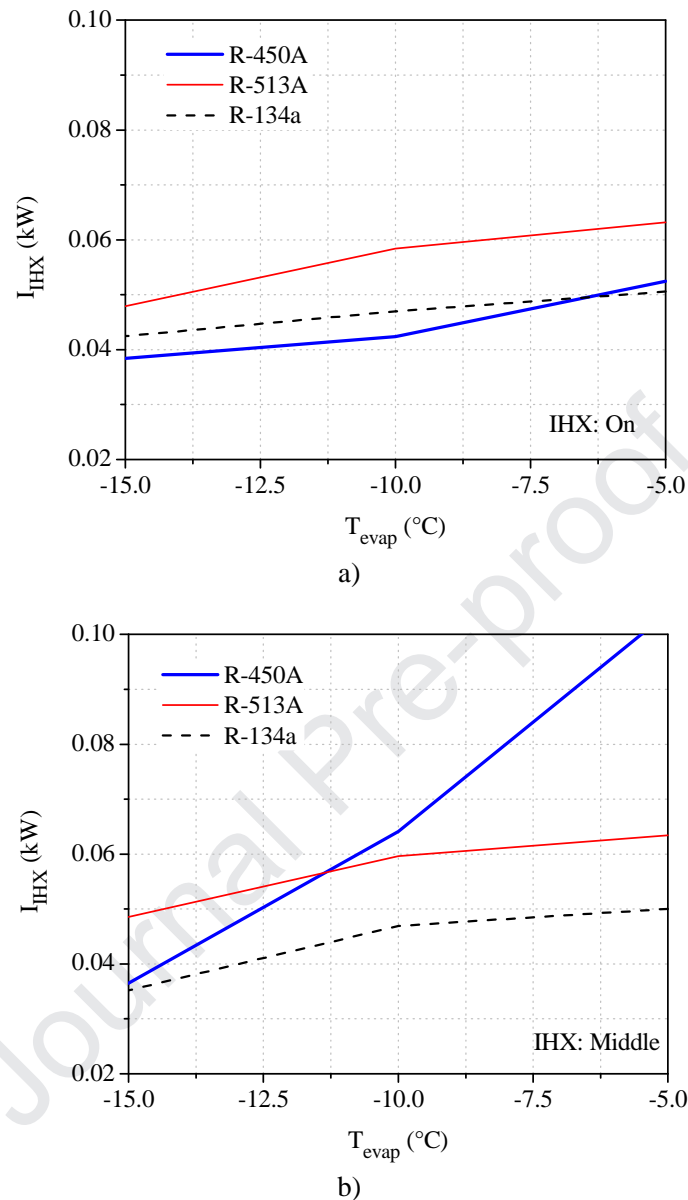
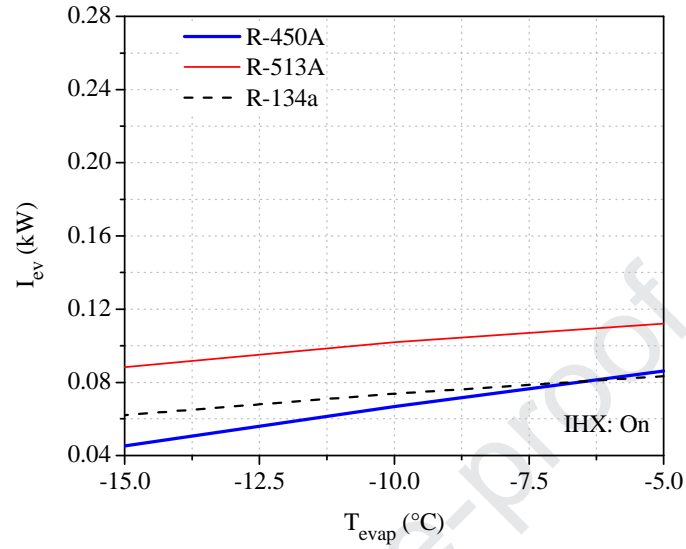


Figure 8. Irreversibilities in the IHX for each operational mode in the installation.

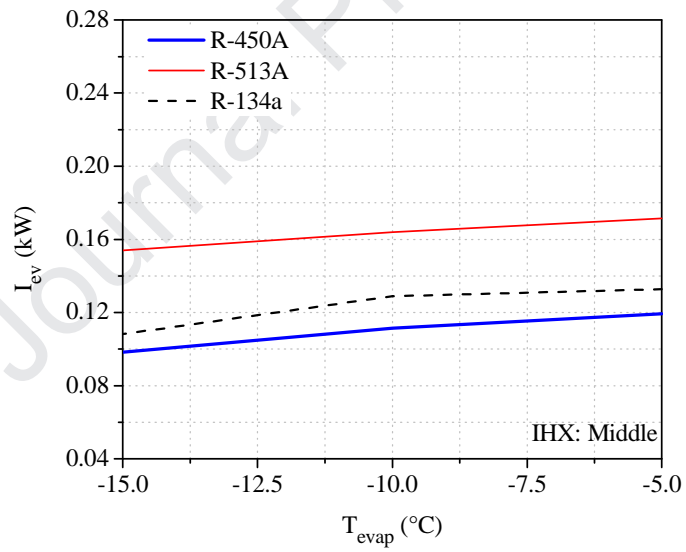
Figure 9 shows the irreversibilities in the expansion valve. For the three operation modes, the irreversibilities are increased for each of the three refrigerants considered. As the evaporation temperature increases, the subcooling decreases, and it causes the entropy at the inlet of the expansion valve to grow, and hence the irreversibility also grows.

Figure 9a) shows that the refrigerant with the highest increase in the component irreversibilities is R-450A with 47.7%, while R-134a and R-513A barely produced an increase of 25.5% and 21.2%, respectively. Figure 9b) shows that the refrigerant which produces a higher increase in the irreversibility is R-134a, followed by R-450A and R-513A, which show an increase of 18.5%, 12.6% and 10.2%, respectively. In Figure 9c), when the IHX is not working, the irreversibilities produced at the expansion valve are very similar to R-134a and R-450A, where R-513A presents

the highest magnitude irreversibilities. In this operation mode, the increase in the irreversibility for this component is the lowest, as it barely reaches 2.0%, 7.5% and 3.5% for R-450A, R-134a and R-513A, respectively.



a)



b)

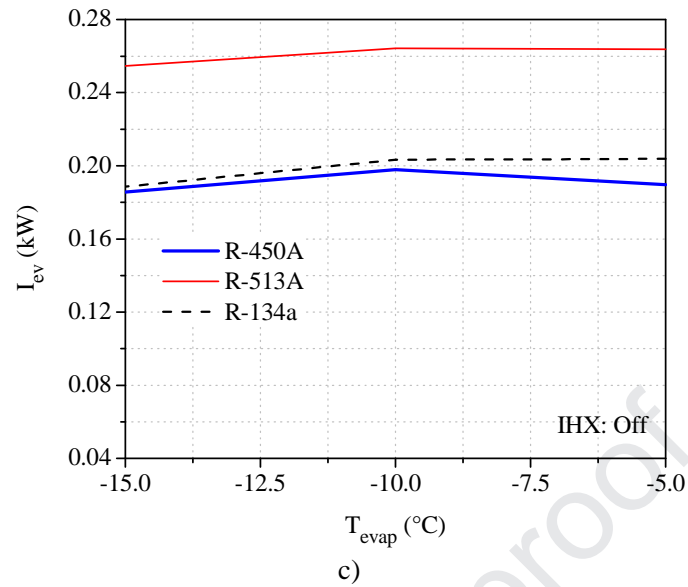
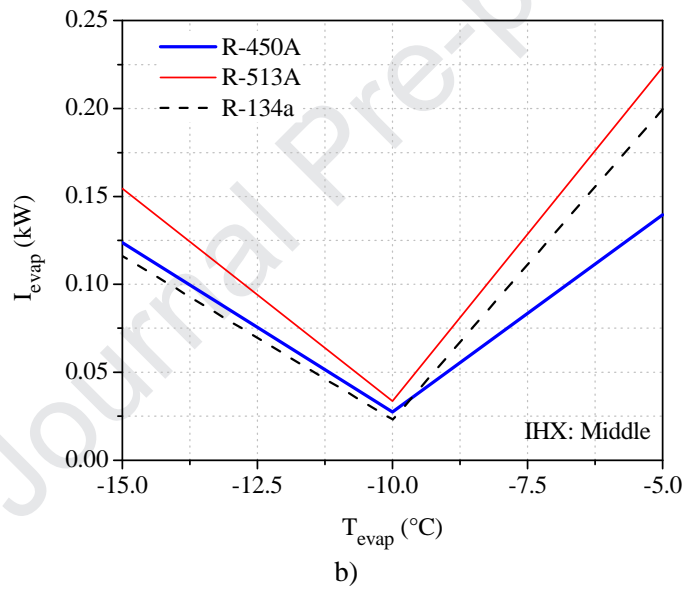
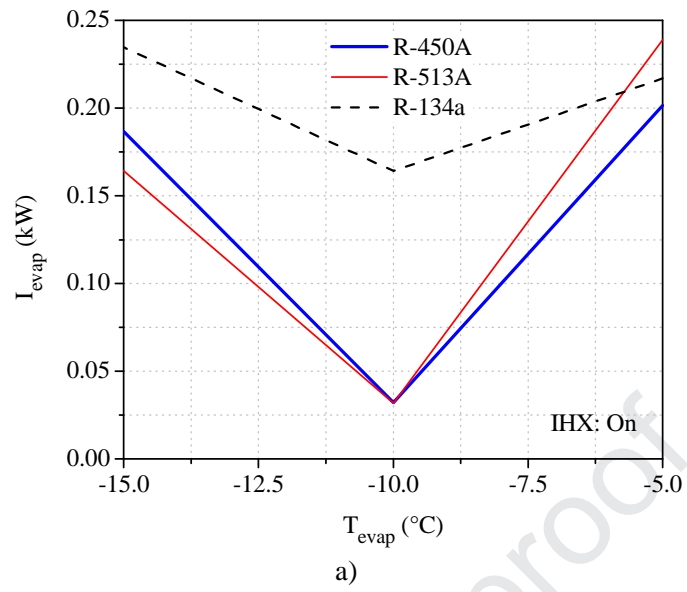


Figure 9. Irreversibilities in the expansion valve for each operational mode of IHX.

Figure 10 presents the irreversibility behavior in the evaporator for each IHX operation level. There is an inflection point in which the irreversibility reached in the component is minimal for all the cases. The reason for this is that, as the evaporation temperature is increased, the superheating reached in the evaporator is not constant. Therefore, the entropy line, which occurs closer to the outlet conditions of the refrigerant in the evaporator, causes that the entropy for both temperatures of -15°C and -5°C to be similar, while at a temperature of -10°C it experiences a decrease.

The influence of the IHX is evident in each of the graphics shown. Figure 10a) shows that R-134a produces major irreversibility in the evaporator while both R-450A and R-513A present a very similar irreversibility optimal value. Additionally, the irreversibility in the evaporator when using R-450A from -10°C to -5°C is lower than it is for R-513A. However, the irreversibility in R-513A from -15°C to -10°C is lower than it is for R-450A. Figure 10b) illustrates how R-513A has superior irreversibility in Middle mode. Therefore, this operation mode affects more to this refrigerant than it does to R-134a and R-450A. In this regard, R-450A produces lower irreversibility in the evaporator from -10°C to -5°C . Figure 10c) depicts a similar behavior to Figure 10b), however in the optimal point, which occurs at -10°C for the three refrigerants and the three IHX operation modes, R-134a shows a slightly lower irreversibility with a value of 5W in comparison with 10 W and 12 W for R-450A and R-513A, respectively.



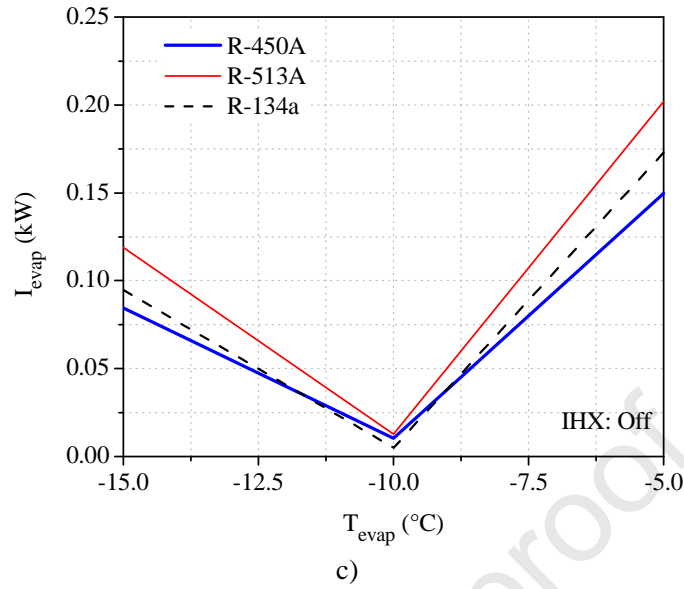


Figure 10. Irreversibilities in the evaporator for each operational mode of IHX.

4.7. Uncertainty analysis

The uncertainty analysis is the estimate of the uncertainties effect on the individual evaluations over the calculated result, [34], and it is used to evaluate the error in the experimental measurements. The uncertainty in the COP, EDR y η_{II} was determined through the root sum squared method (RSS), equation (9).

$$U_Y = \sqrt{\sum_{i=1}^n \left(\frac{\partial U_Y}{\partial X_i} X_i \right)^2} \quad (9)$$

The uncertainty results for each of the parameters above are shown in Appendix 1 in this paper. The data in Table 1 corresponds to the uncertainty of the sensors to measure the temperature, pressure and mass flow variations, and they were used to calculate the uncertainty.

5. CONCLUSIONS

The use of IHX for different operation modes was conducted to find the impact of the effectiveness of this component in the energy performance of the cycle and determine the components with the highest irreversibility depending on the IHX effectiveness. This work analyzes two mixtures with a lower GWP, R-450A and R-513A, and compare them with the current R-134a. The IHX effectiveness was varied to find the effect it has on each component and to know the least efficient components using an analysis by First and Second Law of Thermodynamics. Thus, the conclusions obtained from this work are as follows:

- When the IHX operates in ON mode, R-513A is the refrigerant that shows the best energy performances for temperatures under -5°C . For a configuration with the IHX activated, R-513A is the best option for refrigeration conditions at medium and low temperature.
- If the refrigeration cycle is working with IHX in Middle mode, R-450A is the best option concerning energy performance for refrigeration conditions at medium temperature.

- R-513A is the most affected refrigerant when the installation is working in OFF mode. Hence it is suggested to use this refrigerant only when an IHX is incorporated into the cycle.
- The refrigerant that causes higher irreversibility in the condenser is R-513A, where R-450A presents the lowest irreversibilities in magnitude.
- Based on the exergy analysis for each component, the condenser presents the highest exergy destruction, and therefore, it is the least efficient when using the ON configuration at an evaporation temperature of -5°C .

Based on the study conducted, it can be mentioned that the use of HFC/HFO mixtures is justified in the medium term, as they prove to be competent from an energy and exergy point of view compared to R-134a results. Moreover, the IHX operation mode is an important factor in understanding the behavior of the components when the installation must reduce its capacity to refrigerate.

Finally, as practical challenges when adding the IHX, it can be concluded that, the use of an IHX into existing systems must consider the additional refrigerant charge required, that would result in a slightly higher cost of refrigerant and higher refrigerant leakage. Moreover, minor modifications in the refrigeration system as more space needed and the utilization of ball valves for bypassing the IHX or regulating the IHX effectiveness must be taken into account. The derived effects of the IHX can be an essential factor, as the additional pressure drops (especially in the suction line), the variation of the compressor power consumption and discharge temperature due to the increase of total superheating. Attending to the experimental results presented in this article, for the conditions tested, the electricity consumption is only increased effect for the R-513A alternative.

ACKNOWLEDGMENTS

Vicente Pérez-García would like to thank Secretaría de Educación Pública which, through PRODEP (Programa para el Desarrollo Profesional Docente), financed the academic stay at Universitat Jaume I via the support obtained in the call for “Apoyo a la Incorporación de NPTC 2017”.

Adrián Mota-Babiloni would like to thank the financial support from the Spanish Government through the aid FJCI-2016-28324 and Banco Santander, and Universitat Jaume I for the mobility grant, “Becas Iberoamérica. Santander Universidades. Convocatoria 2017/2018”

APENDIX 1

Table A. Uncertainty for R-134a

IHX operational mode	Parameter	Evaporation Temperature		
		-5°C	-10°C	-15°C
On	COP	3.153 ± 0.092	2.345 ± 0.089	1.699 ± 0.088
	η_{II}	0.3832 ± 0.012	0.3487 ± 0.014	0.290 ± 0.015
	EDR	1.61 ± 0.084	1.868 ± 0.114	2.448 ± 0.127
Middle	COP	3.02 ± 0.086	2.257 ± 0.082	1.599 ± 0.078
	η_{II}	0.3748 ± 0.010	0.3334 ± 0.013	0.2768 ± 0.014
	EDR	1.668 ± 0.083	1.999 ± 0.114	2.613 ± 0.182
Off	COP	2.862 ± 0.075	2.107 ± 0.071	1.567 ± 0.067
	η_{II}	0.3515 ± 0.010	0.3114 ± 0.011	0.2671 ± 0.012
	EDR	1.845 ± 0.083	2.211 ± 0.114	2.744 ± 0.164

Table B. Uncertainty for R-450A

IHX operational mode	Parameter	Evaporation Temperature		
		-5°C	-10°C	-15°C
On	COP	3.175±0.096	2.369±0.099	1.7816±0.102
	η_{II}	0.3885±0.013	0.3522±0.015	0.301±0.016
	EDR	1.574±0.085	1.839±0.123	2.333±0.135
Middle	COP	2.78±0.091	2.105±0.087	1.5684±0.084
	η_{II}	0.3544±0.012	0.3175±0.014	0.2975±0.015
	EDR	1.822±0.099	2.15±0.135	2.6234±0.154
Off	COP	2.86±0.079	2.125±0.073	1.573±0.081
	η_{II}	0.3496±0.01092	0.3132±0.01139	0.2721±0.012
	EDR	1.86±0.08938	2.193±0.1162	2.7146±0.132

Table C. Uncertainty for R-513A

IHX operational mode	Parameter	Evaporation Temperature		
		-5°C	-10°C	-15°C
On	COP	3.09±0.076	2.451±0.075	1.869±0.074
	η_{II}	0.3808±0.011	0.357±0.012	0.3137±0.013
	EDR	1.626±0.073	1.801±0.092	2.188±0.131
Middle	COP	3.026±0.071	2.337±0.068	1.792±0.067
	η_{II}	0.3725±0.010	0.3407±0.011	0.3025±0.011
	EDR	1.685±0.072	1.935±0.092	2.306±0.128
Off	COP	2.743±0.059	2.121±0.057	1.614±0.054
	η_{II}	0.3302±0.008	0.3083±0.009	0.2728±0.009
	EDR	2.028±0.077	2.244±0.095	2.666±0.129

REFERENCES

- [1] A. Mota-Babiloni, P. Makhnatch, R. Khodabandeh, 2018, Recent investigations in HFC substitution with lower GWP synthetic alternatives: Focus on energetic performance and environmental impact, *International Journal of Refrigeration*, 82, pp. 288-301.
- [2] G. Myhre, D. Shindell, F.-M. Bréon, W. Collins, J. Fuglestedt, J. Huang, D. Koch, J.-F. Lamarque, D. Lee, B. Mendoza, T. Nakajima, A. Robock, G. Stephens, T. Takemura and H. Zhang, 2013: Anthropogenic and Natural Radiative Forcing. In: *Climate Change 2013: The Physical Science Basis Contribution of Working Group I to the Fifth Assessment Report of the Intergovernmental Panel on Climate Change* [Stocker, T.F., D. Qin, G.-K. Plattner, M. Tignor, S.K. Allen, J. Boschung, A. Nauels, Y. Xia, V. Bex and P.M. Midgley (eds)]. Cambridge University Press, Cambridge, United Kingdom and New York, NY, USA, page. 714.
- [3] European Parliament and Council of the European Union, Regulation (EU) No. 517/2014 of the European Parliament and the council on fluorinated greenhouse gases. *Off. J. Eur. Union*, 2014:195-230.
- [4] United Nations Environment Programme (UNEP), 2016, Kigali, Rwanda, The Kigali amendment to the Montreal protocol: another global commitment to stop climate change, available

in: <https://www.unenvironment.org/news-and-stories/news/kigali-amendment-montreal-protocol-another-global-commitment-stop-climate>

[5] W. Goetzler, T. Sutherland, M. Rassi, J. Burgos, 2014, Research & Development Road for Next-Generation Low Global Warming Potential Refrigerants, U.S. Department of Energy, Appendix C, page 49 and 50, available in: <https://www.energy.gov/sites/prod/files/2014/12/f19/Refrigerants%20Roadmap%20Final%20Report%202014.pdf>

[6] V. Pérez-García, Juan M. Belman-Flores, José L. Rodríguez-Muñoz, Víctor H. Rangel-Hernández, A. Gallegos-Muñoz, 2017, Second Law Analysis of a Mobile Air Conditioning system with Internal Heat Exchanger Using Low GWP Refrigerants, *Entropy*, 19, 175, doi: 10.3390/e19040175.

[7] En378-1:2000, Refrigerating systems and heat pumps safety and environmental, requirements, Part 1: basic requirements, definitions, classification and selection criteria.

[8] Z. Meng, H. Zhang, J. Qiu and M. Lei, Theoretical analysis of R1234ze(E), R152a, and R1234ze(E)/R152a mixtures as replacements of R134a in vapor compression system, 2016, *Advances in Mechanical Engineering*, Vol. 8 (11), pp. 1-10.

[9] M. Direk, A. Kelesoglu, A. Akin, 2017, Theoretical Performance Analysis of an R1234yf refrigeration cycle based on the effectiveness of internal heat exchanger, *Hittite Journal of Science and Engineering*, 4 (1), pp. 23-30.

[10] J. Navarro-Esbrí, Francisco Molés, Ángel Barragán-Cervera, 2013, Experimental análisis of the internal heat exchanger influence on a vapour compression system performance working with R1234yf as a drop-in replacement for R134a, *Applied Thermal Engineering*, 59, pp. 153-161.

[11] A. Mota-Babiloni, Joaquín Navarro-Esbrí, Ángel Barragán, Francisco Molés, Bernardo Peris. 2014, Drop-in energy performance evaluation of R1234yf and R1234ze(E) in a vapor compression system as R134a replacements, *Applied Thermal Engineering*, 71, pp. 259-265.

[12] A. G. Devecioglu, V. Oruç, 2018, Improvement on the energy performance of a refrigeration system adapting a plate-type heat exchanger and low-GWP refrigerants as alternatives to R134a, *Energy*, 155, pp. 105-116.

[13] J. Gill, J. Singh, S. Olayinka Ohunakin, S. Demola S. Adelekan, 2018, Exergy analysis of vapor compression refrigeration system using R450A as a replacement of R134a, *Journal of Thermal Analysis and Calorimetry*, 136, pp. 857-872.

[14] A. Mota-Babiloni, J.M. Belman-Flores, P. Makhnatch, J. Navarro-Esbrí, J.M. Barroso-Maldonado, 2018, Experimental exergy analysis of R513A to replace R134a in a small capacity refrigeration system, *Energy*, 162, pp. 99-110.

[15] M. Yang, H. Zhang, Z. Meng, Y. Qin, 2019, Experimental study on R1234yf/R134a mixture (R513A) as R134a replacement in a domestic refrigerator, *Applied Thermal Engineering*, 146, pp. 540-547.

[16] P. Makhnatch, A. Mota-Babiloni, A. López-Belchí, R. Khodabandeh, 2019, R450A and R513A as lower GWP mixtures for high ambient temperature countries: Experimental comparison with R134a, *Energy*, 166, pp. 223-235.

- [17] A. López-Belchí, 2019, Assessment of a mini-channel condenser at high ambient temperatures based on experimental measurements working with R134a, R513A and R1234yf, *Applied Thermal Engineering*, 155, pp. 341-353.
- [18] A. Mota-Babiloni, J. Navarro-Esbrí, A. Barragán-Cervera, F. Molés, Bernardo Peris, 2015, Experimental study of an R1234ze(E)/R134a mixture (R450A) as R134a replacement, *International Journal of Refrigeration*, 51, pp. 52-58.
- [19] A. Mota-Babiloni, J. Navarro-Esbrí, V. Pascual-Miralles, A. Barragán-Cervera, A. Maiorino, 2019, Experimental influence of an internal heat exchanger (IHX) using R513A and R134a in vapor compression system, *Applied Thermal Engineering*, 147, pp. 482-491.
- [20] J.M. Belman-Flores, V.H. Rangel-Hernández, S. Usón, C. Rubio-Maya, 2017, Energy and exergy analysis of R1234yf as drop-in replacement for R134a in a domestic refrigeration system, *Energy*, 132, pp. 116-125.
- [21] M. Araz, A. Güngör and A. Hepbasli, 2015, Experimental Exergetic Performance Evaluation of an Elevator in Air Conditioner Using R-1234yf, *Int. Journal of Engineering and Technology*, Vol. 7(3), pp. 254-260.
- [22] M. Direk, M. Selcuk Mert, E. Soylu, F. Yüksel, 2019, Experimental Investigation of an Automotive Air Conditioning System Using R444A and R152a Refrigerants as Alternatives of R134a, *Strojnicki vestnik Journal of Mechanical Engineering*, Vol. 65 (4), pp. 212-218.
- [23] H. Cho, Ch. Park, Experimental investigation of performance and exergy analysis of automotive air conditioning system using refrigerant R1234yf at various compressor speeds, *Applied Thermal Engineering*, 101, pp. 30-37.
- [24] M. Direk, M.S. Mert, F. Yüksel, A. Kelesoglu, 2018, Exergetic Investigation of R1234yf Automotive Air Conditioning System with Internal Heat Exchanger, *International Journal of Thermodynamics*, Vol. 21 (2), pp. 103-109.
- [25] E.W. Lemmon, M.L. Huber, M.O. McLinden., REFPROP, 2014, NIST Standard Reference Database 23 v.9.1. National Institute of Standards, Gaithersburg, MD, USA.
- [26] J.M. Mendoza-Miranda, A. Mota-Babiloni, J.J. Ramírez-Minguela, V.D. Muñoz-Carpio, M. Carrera-Rodríguez, J. Navarro-Esbrí, C. Salazar-Hernández, 2016, Comparative evaluation of R1234yf, R1234ze(E) and R450A as alternatives to R134a in a variable speed reciprocating compressor, *Energy*, 114, pp. 753-766.
- [27] P. Makhnatch, A. Mota-Babiloni, R. Khodabandeh, 2017, Experimental study of R450A drop-in performance in an R134a small capacity refrigeration unit, *International Journal of Refrigeration*, 84, pp. 26-35.
- [28] G., R. Kumar, 2018, Computational energy and exergy analysis of R134a, R1234yf, R1234ze and their mixtures in vapour compression system, *Ain Shams Engineering Journal*, 9, pp. 3229-3237.
- [29] G. Sachdeva, V. Jain, 2016, Comparative exergy analysis of vapor compression refrigeration system using alternative refrigerants, *International Scholarly and Scientific Research & Innovation* 10(6), pp. 1081-1088.

[30] J.U. Ahamed, R. Saidur, H.H. Masjuki, 2011, A review on exergy analysis of vapor compression refrigeration system, *Renewable and Sustainable Energy Reviews*, 15 (3), pp. 1593-1600.

[31] L. Tzong-Shing, 2010, Second Law Analysis to improve the energy efficiency of screw liquid chillers, *Entropy*, 12, pp. 375-389; doi: 10.3390/e12030375.

[32] SA Said, B. Ismail, 1994, Exergetic assessment of the coolants HCFC123, HFC134a, CFC11 and CFC12, *Energy*, 19, pp. 1181-1186.

[33] SA Klein, *Engineering Equation Solver*, Version 6.883, Middleton, WI: F-Chart Software, 2003.

[34] R. J. Moffat, 1988, Describing the Uncertainties in Experimental Results, *Experimental Thermal and Fluid Science*.

Highlights:

- The use of an IHX in different activation modes produces an increase in the COP
- The activation of an IHX promotes the highest exergy destruction in condenser
- Use of R-513A is suggested only if an IHX is incorporated in a refrigeration cycle
- Use of an IHX can reduce exergy destruction up to 22.2%

Journal Pre-proof